ISSN 0006-2979, Biochemistry (Moscow), 2019, Vol. 84, No. 10, pp. 1151-1165. © Pleiades Publishing, Ltd., 2019.
Russian Text © The Author(s), 2019, published in Biokhimiya, 2019, Vol. 84, No. 10, pp. 1421-1436.
Originally published in Biochemistry (Moscow) On-Line Papers in Press, as Manuscript BM19-041, August 26, 2019.

Protonophoric and Photodynamic Effects of Fluorescein Decyl(triphenyl)phosphonium Ester on the Electrical Activity of Pond Snail Neurons

L. B. Popova[1], A. L. Kamysheva[1], T. I. Rokitskaya[1], G. A. Korshunova[1], R. S. Kirsanov[1], E. A. Kotova[1], and Y. N. Antonenko[1,a]*

[1]*Belozersky Institute of Physico-Chemical Biology, Lomonosov Moscow State University, 119991 Moscow, Russia*
[a]*e-mail: antonen@genebee.msu.ru*

Received February 18, 2019
Revised June 6, 2019
Accepted June 17, 2019

Abstract—Uncouplers of oxidative phosphorylation in mitochondria, which have been essential in elucidating the basic principles of cell bioenergetics, have recently attracted a considerable interest as compounds with therapeutic, e.g., neuroprotective, properties. Here, we report the effect of mitofluorescein (mitoFluo), a new protonophoric uncoupler representing a conjugate of fluorescein with decyl(triphenyl)phosphonium, on the electrical activity of neurons from *Lymnaea stagnalis*. Incubation with mitoFluo in the dark led to a decrease in the absolute value of the resting membrane potential of the neurons and alterations in their spike activity, such as spike broadening, spike amplitude reduction, and increase in the spike frequency. Prolonged incubation at high (tens micromoles) mitoFluo concentrations resulted in complete suppression of neuronal electrical activity. The effect of mitoFluo on the neurons was qualitatively similar to that of the classical mitochondrial uncoupler carbonyl cyanide *m*-chlorophenylhydrazone (CCCP) but manifested itself after much longer incubation and at higher concentrations. The distinctive feature of mitoFluo is its light-induced effect on the electrical activity of neurons. Changes in the parameters of the neuronal activity upon illumination in the presence of mitoFluo were similar to the light-induced effects of the well-known photosensitizer Rose Bengal, although less pronounced. It was suggested that the effects of mitoFluo on the electrical activity of neurons, both as a mitochondrial uncoupler and a photosensitizer, are mediated by the changes in the cytoplasmic calcium concentration.

DOI: 10.1134/S0006297919100043

Keywords: neuron, membrane potential, action potential, uncoupler, protonophore, mitochondria, Ca^{2+}

The restoration of the blood flow (reperfusion) after a period of reduced blood supply (ischemia) causes significant brain tissue damage associated to a large extent with the formation of reactive oxygen species (ROS). The protective effect of mitochondrial uncouplers was demonstrated in a number of ischemia-reperfusion models [1-3] and other types of brain injury [4], which was supposedly due to the ability of oxidative phosphorylation uncouplers to suppress ROS generation because of its dependence on the mitochondrial membrane potential [2, 5-7]. Uncouplers cause the dissipation of the proton electrochemical potential at the inner mitochondrial membrane via the membrane proton transfer [8], thus disrupting the coupling between the electron transport in the respiratory chain and ATP synthesis [9, 10].

Along with potential use of uncouplers in the treatment of obesity and oxidative stress-related disorders (including neurodegenerative diseases), recently interest in uncouplers has been associated with their antimicrobial and anticancer activities. In this connection, several research groups have attempted to generate uncouplers with new beneficial properties. In particular, we synthesized and investigated uncouplers based on the known fluorophore fluorescein [4, 11, 12]. A distinguishing feature of these compounds is bright fluorescence that allows

Abbreviations: BLM, bilayer lipid membrane; CCCP, carbonyl cyanide *m*-chlorophenylhydrazone; CGC, cerebral giant cell; DNP, 2,4-dinitrophenol; DPhPC, diphytanoyl phosphatidylcholine; FCCP, carbonyl cyanide *p*-trifluoromethoxyphenylhydrazone; mitoFluo, mitofluorescein, {10-[2-(3-hydroxy-6-oxoxanthen-9-yl)benzoyl]oxidecyl}(triphenyl)phosphonium bromide; RMP, resting membrane potential; ROS, reactive oxygen species.

* To whom correspondence should be addressed.

to monitor their intracellular location. However, the drawback of the photoactive fluorescein derivatives is that similarly to many other dyes, they display the photodynamic activity, i.e., initiate light-induced cell damage in the presence of oxygen. Snail neurons are a good model for investigating the effect of uncouplers on the electrical activity of nerve cells. We demonstrated in [13] that the classical uncouplers, such as carbonyl cyanide *m*-chlorophenylhydrazone (CCCP) and 2,4-dinitrophenol (DNP), caused depolarization of the neuronal plasma membrane and broadening of spikes; moreover, these effects were likely mediated by the uncoupler action on the neuron mitochondria. It has been also found that the classical uncouplers CCCP [14] and carbonyl cyanide *p*-trifluoromethoxyphenylhydrazone (FCCP) [14, 15] depolarize the plasma membrane of cultured neurons and isolated nerve endings. Here, we conducted a comparative study of the effects of mitofluorescein (mitoFluo), a new uncoupler representing a conjugate of fluorescein with decyl(triphenyl)phosphonium [12], and the conventional uncoupler CCCP on the electrical activity of neurons from the pond snail *Lymnaea stagnalis*. The effect of mitoFluo on the spike frequency and shape was investigated in the dark and upon illumination. It was demonstrated that different types of snail neurons displayed different sensitivity to the action of uncouplers.

MATERIALS AND METHODS

Most reagents used in the study including CCCP were purchased from Sigma (USA). MitoFluo, a conjugate of fluorescein and decyl(triphenyl)phosphonium, was synthesized as described previously [12] in two stages as shown in the scheme. At the first stage, 1,10-dibromodecane (7.2 mmol) and triphenylphosphine (4.7 mmol) were dissolved in benzene and heated at 80°C for 20 h in a tightly sealed flask. The mixture was then cooled down to room temperature and evaporated to dryness. Next, the product [10-bromodecyl(triphenyl)phosphonium bromide] was isolated by multiple rounds of precipitation from dichloromethane by diethyl ester followed by purification by column chromatography on MN Kieselgel 60 (240-400 mesh) using ethanol– dichloromethane (1 : 5, v/v) as an eluent. At the second stage, 10-bromodecyl(triphenyl)phosphonium bromide solution (2 mmol) in a minimal volume of CH_2Cl_2 was added to fluorescein (2 mmol) and sodium carbonate (3.8 mmol) in 40 ml of dimethylformamide (DMFA) and heated to 60°C for 3 h. The reaction mixture was then cooled down to room temperature and diluted with 100 ml of CH_2Cl_2. The reaction product {10-[2-(3-hydroxy-6-oxoxanthen-9-yl)benzoyl]oxidecyl}(triphenyl)phosphonium bromide (mitoFluo) was extracted with dichloromethane and purified by column chromatography on a silica gel using ethanol–dichloromethane (1 : 5, v/v) as an eluent.

Electrophysiological experiments were carried out in neurons from the pond snail *L. stagnalis*. The snails were grown in a laboratory aquarium with fresh water. The central nervous system consisting of the central ring and buccal ganglia was surgically removed and transferred into a silicon (Silgard)-lined bath filled with standard saline containing (mM): 44.0 NaCl, 2.0 KCl, 4.0 $CaCl_2$, 1.5 $MgCl_2$, 10.0 HEPES (pH 7.6). In order to ease the penetration of recording electrodes into the neurons, the surface of the ganglia was first softened with 0.1% pronase solution (protease Type XIV; Sigma) for 10 min. After washing out the enzyme, the cerebral commissure was cut. To see the neurons, the ganglia were disrupted on the bath bottom with miniature needles. The functions of identified neurons have been well studied and described [16]. The studied neurons were cerebral giant cells (CGCs), buccal neurons B1, B2, and B4) [17], and large neurons from the pedal and visceral ganglia. The neuronal activity was recorded using intracellular glass microelectrodes filled with 2 M KCl (tip resistance, 20-60 MΩ). In some experiments, two microelectrodes were introduced into a neuron under visual control; one of them served for the current injection, and the other – for measuring the potential shift. It is known that isolated molluscan ganglia can maintain their functions in the absence of afferent and efferent organs for a long period

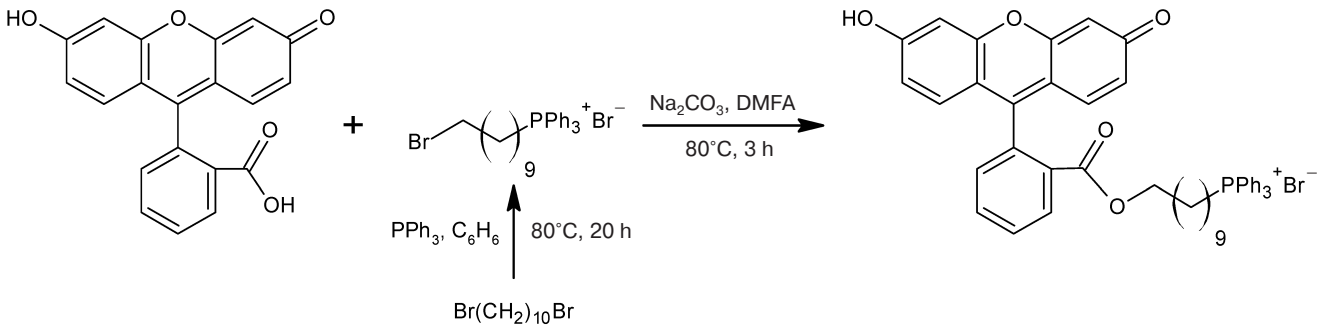

Scheme

of time (over 10 h). An aliquot (5-50 μl) of the effector stock solution was added to the bath (2 ml) with a pipette within 20-30 s. In the washing out experiments, the mitoFluo solution in the 2-ml bath was gradually replaced with saline (20 ml) using a 0.5-ml pipette, resulting in ~6000-fold decrease in the initial mitoFluo concentration.

Neurons were illuminated with a TDS-P005L8011 light-emitting diode (white light 140″, 350 lm, 5 W) via fiber-optic lightguide.

Membrane potential was measured with an AxoClamp 2B dual-channel biopotential amplifier (Axon Instruments, USA) that allowed current injection through the microelectrode. The data were registered with a computer using a DigiData 1200 series analog to digital converter and the pCLAMP 8 program (Molecular Devices, USA). Statistical processing of the data was carried out with the SigmaPlot 9.0 program (Systat Software, USA). The RMP of the neurons, spike amplitude, spike half-width, membrane depolarization and repolarization slopes during the spike, and average spike frequency were measured to provide quantitative evaluation of the effects of studied compounds on cell functioning. These parameters were measured and averaged over the time period of 1 min before the compound addition and for 1 min after the addition, when the neuron response was most pronounced. In some experiments with the high-frequency action potential and uniform cell functioning, the measuring time was reduced to 30 s. The statistical significance of pair measurements before and after compound addition was estimated with the Student's *t*-test. In the cases when data did not display normal distribution, we used the non-parametric Wilcoxon *t*-test.

Rat liver mitochondria were isolated as described in [18].

Bilayer lipid membrane (BLM) was formed from a 2% diphytanoyl phosphatidylcholine (DPhPC; Avanti Polar Lipids, USA) solution in decane on an aperture (diameter, 0.5 mm) in a partition separating Teflon chamber filled with the buffer solution (100 mM KCl, 10 mM Tris, pH 7.4) [19]. Gramicidin A (Sigma, USA) was added as a concentrated ethanol solution to the aqueous solution on both sides of the membrane and stirred thoroughly for 15 min. MitoFluo was added as a concentrated ethanol solution to the aqueous solution at the *trans*-side of the membrane (*cis*-side was the side exposed to illumination) and stirred thoroughly for 20 min. All experiments were carried out at room temperature (23-25°C). Electric current through the BLM was recorded at a fixed potential. The potential difference was applied to the Ag/AgCl electrodes placed into the Teflon chamber. The current was recorded with a Keithley 428 amplifier (Keithley Instruments, USA), digitized with a NI-DAQmx driver (National Instruments, USA), and analyzed using the WinWCP Strathclyde Electrophysiology Software created by John Dempster (University of Strathclyde, Glasgow, UK). BLMs were continuously illuminated with a halogen lamp (NovaFlex; World Precision Instruments, Inc., USA) with a power density of 0.77 W/cm^2 for 60 s. Glass filter cutting off light with the wavelength <500 nm was placed between the lamp and the chamber.

RESULTS AND DISCUSSION

Effect of the classical uncoupler CCCP on the electrical activity of isolated *L. stagnalis* ganglion cells. First, we studied the effect of the conventional mitochondrial uncoupler CCCP on the electrical activity of neurons in the isolated *L. stagnalis* ganglia. Motor neurons of the buccal ganglia (B1, B2, B4) involved in the buccal muscles control, cerebral giant cells (CGCs, serotoninergic modulating neurons) regulating the functions of the buccal cells, and the cells of the visceral and pedal ganglia were examined. In total, 13 experiments were conducted, in which we recorded the activity of 10 CGCs, 10 buccal, 7 visceral, and 2 pedal neurons. Buccal neurons form the central pattern generator (CPG) responsible for the generation of buccal muscles rhythmic movements involved in snail feeding. The activity of this driver can be evaluated from the rhythmic alternation between the bursts of spike activity and periods of inhibition of the B1, B2, and B4 neurons [16]. CGC does not belong to CPG and does not display the rhythmic activity. Instead, it modulates intensity of the central pattern generator [17]. Simultaneous recordings of the electrical activity of the B1 neuron and CGC in the isolated snail ganglion are presented in Figs. 1 and 2. Prolonged (30-60 min) monitoring of the activity of these cells in the control demonstrated that their membrane potential measured between the spikes varied within the range of 5 mV.

Depolarization of the neuronal membrane and significant changes in the spike activity of neurons were observed shortly after CCCP addition (Figs. 1a, 1b and 2a, 2b); the increase in the membrane potential occurred after a lag-period, which depended on the CCCP concentration (Figs. 1c, 1f and 2c, 2f). For all the investigated neurons, it was possible to select the uncoupler concentration that caused membrane depolarization, as it has been reported for the buccal cells in our previous work [13]. In some cases, slight hyperpolarization of the plasma membrane was observed prior to depolarization (Figs. 1c and 2f).

In addition to depolarization, we also revealed an increase in the frequency of the action potential generation in the presence of CCCP (Figs. 1d, 1g, and 2d, 2g). At the same time, a decrease in the amplitude and broadening of spikes were observed (Figs. 1e, 1h, and 2e, 2h). Neuron silencing (complete suppression of spike activity) in the buccal cells occurred at a significantly lower

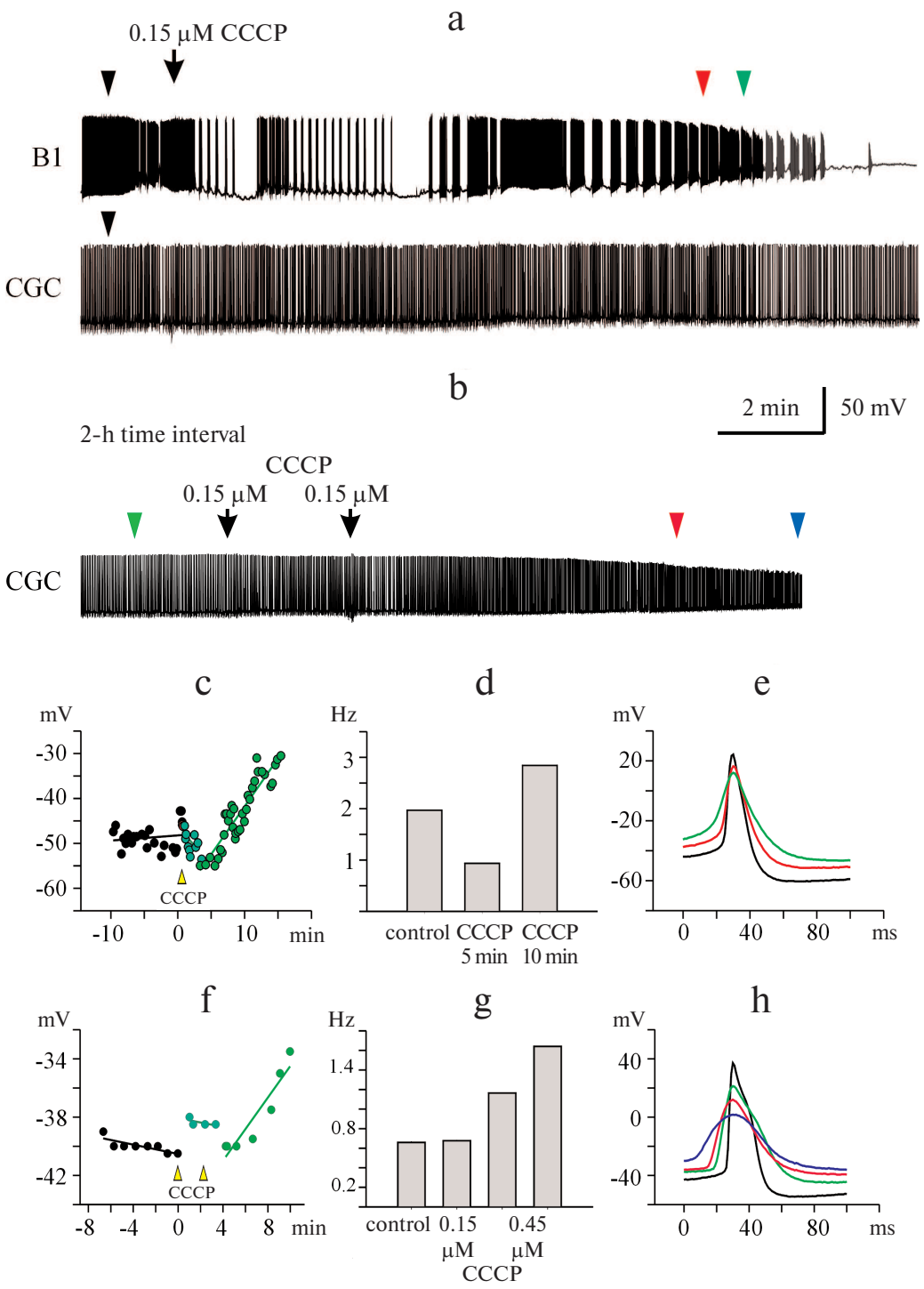

Fig. 1. Effect of submicromolar CCCP concentrations on spontaneous activity of pond snail neurons. a) CCCP at a concentration of 0.15 μM caused depolarization of the plasma membrane and increased action potential frequency followed by the silencing of the buccal neuron B1 but did not affect the activity of the CGC. b) Exposure of the CGC to 0.15 μM CCCP for 2 h only slightly affected its functions. An increase in the CCCP concentration to 0.45 μM resulted in the membrane depolarization, an increase in the action potential frequency, and subsequent CGC silencing. c-e) Resting membrane potential (RMP), average spike frequency, and superposition of action potentials, respectively, of the buccal neuron B1. f-h) RMP, average spike frequency, and superposition of action potentials, respectively, of the CGC. c, f) The moments of the first (c) and second (f) addition of CCCP were considered as time points 0 [marked with black arrows in panels (a) and (b)]. g) Average spike frequency in the presence of 0.15 μM CCCP over the time period of 2 h did not differ from the control one. The third and the fourth bars show average spike frequency over the time intervals 0-5 and 5-10 min following the third addition of CCCP. e, h) Positions of spikes in the recordings presented in panels (a) and (b) are shown with arrowheads of the corresponding color. Control spikes are shown in black.

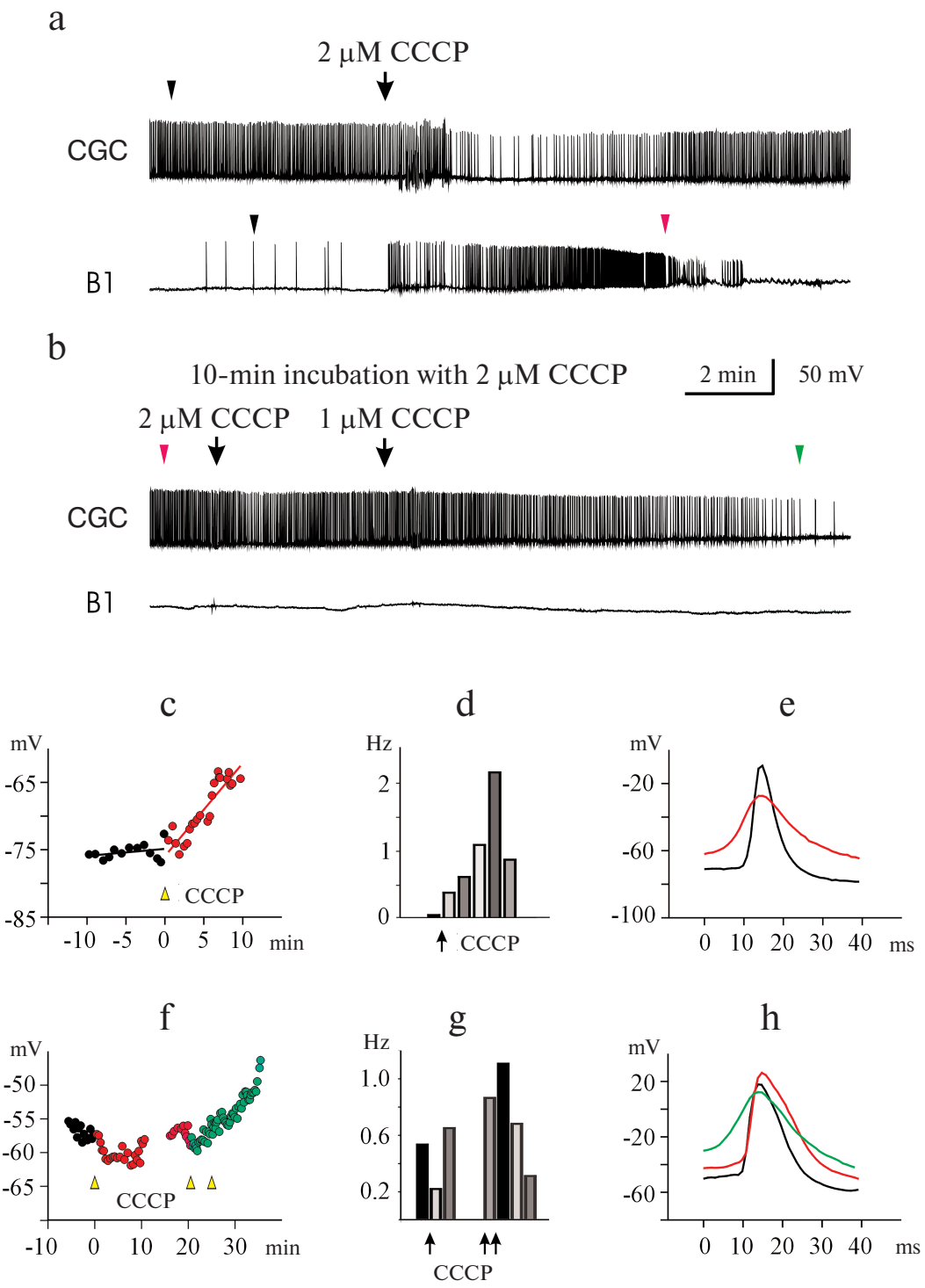

Fig. 2. CCCP at micromolar concentrations affects spontaneous activity of buccal neuron B1 and CGC. a) CCCP (2 μM) caused depolarization of the plasma membrane and an increase in the action potential frequency in the B1 neuron, followed by neuron silencing. In the CGC, initial membrane depolarization and slowing of the spike activity were followed by lesser depolarization and gradual increase in the action potential frequency. b) Increasing the CCCP concentration to 5 μM resulted in further depolarization of the CGC membrane and increase in the spike frequency, followed by complete inhibition of the spike activity, while membrane potential of the B1 neuron changed only slightly. c-e) RMP, average spike frequency, and superposition of action potentials of the neuron B1, respectively. f-h) RMP, average spike frequency, and superposition of action potentials of the CGC, respectively. c, f) The moments of the first addition of CCCP were considered as time point 0 [marked with black arrow in panel (a)]. d, g) Histograms of the average spike frequency within the time intervals of 1.5 and 5 min, respectively. e, h) Positions of the spikes in the recordings presented in panels (a) and (b) are shown with arrowheads of the corresponding color. Control spikes are shown in black.

uncoupler concentration than in the CGCs. Significant changes in the parameters of electrical activity of buccal cells were observed after the addition of 0.15 μM CCCP to the bath solution.

At a concentration of 0.45 μM, CCCP caused depolarization of the CGC plasma membrane (Fig. 1f) and increased the average frequency of the spike activity almost 2-fold (Fig. 1g). The average spike frequency of all tested CGCs increased by 33% (from 0.69 to 0.92 Hz) under the action of CCCP ($p = 0.05$ according to paired Student's *t*-test). The data for the buccal neurons and CGCs are presented in Tables 1 and 2. Note that the CCCP-induced increase in the action potential frequency was reported previously for cardiomyocytes in [20].

Figures 1e, 1h and 2e, 2h illustrate the effect of low (from 0.15 μM) and high (from 2 μM) CCCP concentration on the shape of spikes generated by the B1 neurons and CGCs at selected time points (triangles of the corresponding color in Figs. 1a, 1b and 2a, 2b). Gradual spike broadening and decrease in the spike amplitude started simultaneously with the membrane depolarization and reached the maximum before the cell silencing. CCCP decreased the average spike amplitude by 24% in all recorded buccal cells – from 56.52 ± 4.41 mV (control) to 42.82 ± 3.75 mV (Table 1; the data are shown as mean ± standard error; paired *t*-test, $p = 0.027$), and by 7% in the CGCs – from 74.92 ± 1.74 mV (control) to 69.56 ± 2.11 mV (Table 2; paired *t*-test, $p = 0.001$). CCCP also affected the rates of spike depolarization and repolarization. In particular, the maximal rates of spike depolarization and repolarization in buccal cell decreased approximately 2-fold, from 21.92 ± 3.73 and −10.47 ± 1.76 mV/ms, respectively, in the control to 10.22 ± 2.57 and −5.50 ± 1.45 mV/ms, respectively, in the presence of CCCP (paired *t*-test, $p = 0.014$ and 0.011, respectively; Table 1). The maximal rates of spike depolarization and repolarization in CGCs decreased from 17.01 ± 1.29 and −6.10 ± 0.6 mV/ms, respectively, in the control to 12.9 ± 1.23 and

Table 1. Effect of CCCP on the B1, B2, and B4 buccal neurons from the isolated pond snail (*L. stagnalis*) ganglia

Buccal neurons, $n = 10$	Control, mean ± standard error	CCCP, mean ± standard error	Paired Student's *t*-test or Wilcoxon *t*-test	Change in percent
Membrane potential (mV)	−49.88 ± 4.58	−43.48 ± 4.77	$p = 0.011$	depolarization by 9%
Spike amplitude (mV)	56.52 ± 4.41	42.82 ± 3.75	$p = 0.027$	decrease by 24%
Spike width at half maximum (ms)	7.76 ± 1.44	12.35 ± 1.68	$p = 0.005$	broadening by 59%
Maximum rate of spike depolarization (mV/ms)	21.92 ± 3.73	10.22 ± 2.57	$p = 0.014$	slowing down by 46.6%
Maximum rate of spike repolarization (mV/ms)	−10.47 ± 1.76	−5.50 ± 1.45	$p = 0.011$	slowing down by 52.5%
Average spike frequency (Hz)	1.98 ± 0.60	5.65 ± 1.23	$p = 0.002$	increase by 185%

Table 2. Effect of CCCP on CGCs from the isolated pond snail (*L. stagnalis*) ganglia

GCCs, $n = 10$	Control, mean ± standard error	CCCP, mean ± standard error	Paired Student's *t*-test or Wilcoxon *t*-test	Change in percent
Membrane potential (mV)	−59.10 ± 4.56	−52.72 ± 4.17	$p < 0.001$	depolarization by 11%
Spike amplitude (mV)	74.92 ± 1.74	69.56 ± 2.11	$p = 0.001$	decrease by 7%
Spike width at half maximum (ms)	16.44 ± 2.29	18.96 ± 1.86	$p = 0.020$	broadening by 15%
Maximum rate of spike depolarization (mV/ms)	17.01 ± 1.29	12.90 ± 1.23	$p = 0.002$	slowing down by 24%
Maximum rate of spike repolarization (mV/ms)	−6.10 ± 0.60	−3.98 ± 0.35	$p = 0.004$	slowing down by 35%
Average spike frequency (Hz)	0.69 ± 0.06	0.92 ± 0.07	$p = 0.050$	increase by 34%

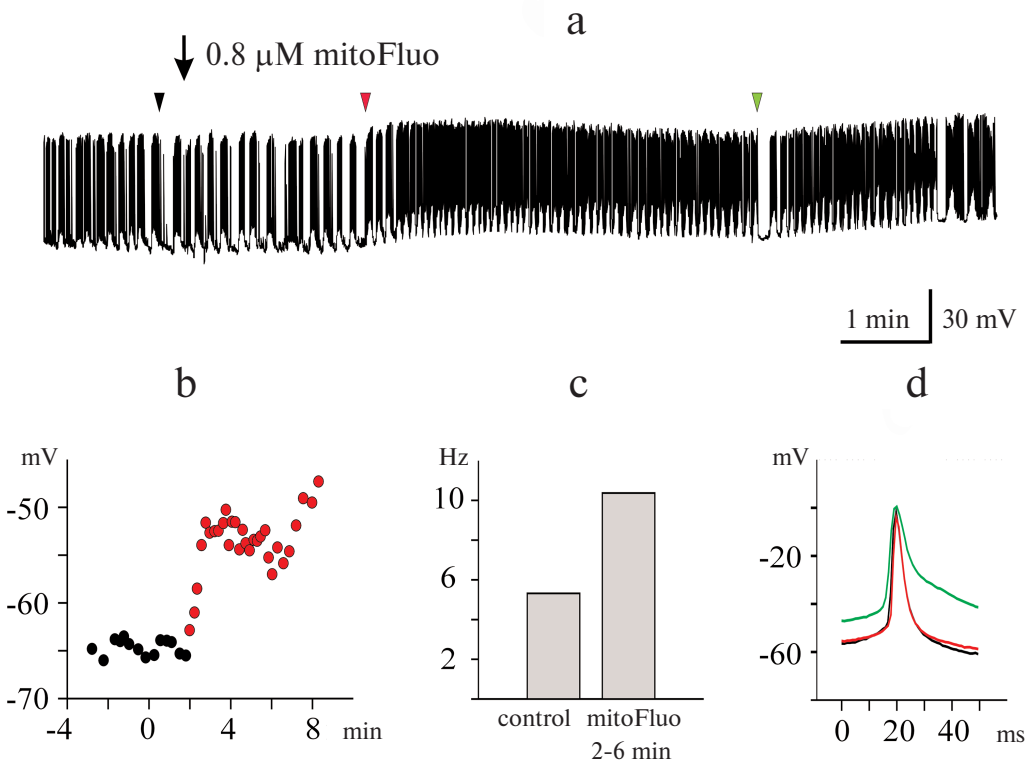

Fig. 3. Effect of low mitoFluo concentration on spontaneous activity of pond snail neurons. a) MitoFluo at a concentration of 0.8 μM caused depolarization of the plasma membrane and increased the action potential frequency in the buccal neuron B4. b) RMP increased rapidly following the addition of mitoFluo. The moment of the mitoFluo addition was considered as time point 0. The latent period of the reaction was ~2 min. c) MitoFluo increased the average action potential frequency 2-fold in comparison with the control. First bar, average spike frequency 4 min prior to the addition of mitoFluo; second bar, average spike frequency 4 min after the addition of mitoFluo. d) Superposition of action potentials. MitoFluo decreased the rates of spike depolarization and repolarization. Positions of the spikes in the recording presented in panel (a) are shown with arrowheads of the corresponding color. Control spike is shown in black.

−3.98 ± 0.35 mV/ms, respectively, in the presence of CCCP (Wilcoxon *t*-test, $p = 0.002$, and paired *t*-test, $p = 0.004$, respectively; Table 2). A 20-30% decrease in the rate of membrane depolarization and repolarization during the spike was accompanied by the spike broadening in the presence of CCCP. Thus, the half-width of action potential in the buccal cells and CGCs increased on average by 59 and 15%, respectively (paired *t*-test, $p = 0.005$ and 0.020, respectively; Tables 1 and 2). An increase in the action potential duration under the action of CCCP and FCCP was observed previously for the neuronal cell culture [14].

We conducted six experiments on the effect of DNP on the electrical activity of different types of pond snail neurons. The number of experiments was insufficient to determine statistically significant differences between the paired measurements before and after DNP addition. However, it should be mentioned that the effect of DNP was similar to the above-described effect of CCCP. The increase in the membrane potential, broadening of spikes, and decrease in the spike amplitude were observed in all experiments, which was in agreement with the previous data on the effect of DNP on the electrical activity of excitable membranes [21, 22]. DNP at a concentration of 150 to 500 μM completely inhibited the electrical activity of neurons. Similarly to CCCP, the time point for the onset of changes in the neuronal activity strongly depended on the DNP concentration (tens of minutes for 150 μM DNP and only minutes for 500 μM DNP). The buccal neurons responded to DNP faster than the CGCs (data not shown).

Effect of mitoFluo on the electrical activity of *L. stagnalis* neurons. In order to investigate the effect of mitoFluo, we conducted 20 experiments and recorded 18 CGCs, 29 buccal neurons, one visceral neuron, and one pedal neuron. Figure 3a shows a typical recording of the activity of buccal neuron B4 in the presence of low mitoFluo concentration. The addition of 0.8 μM mitoFluo induced neuron depolarization (Fig. 3b) and caused an increase in the frequency of action potential generation (Fig. 3c), a decrease in the spike amplitude, and spike broadening (Fig. 3d). The effect of mitoFluo on the neuron functioning was partially retained after washing the ganglia with saline for 2 h.

Figure 4 shows the typical effect of high mitoFluo concentrations vs. control recording of electrical activity

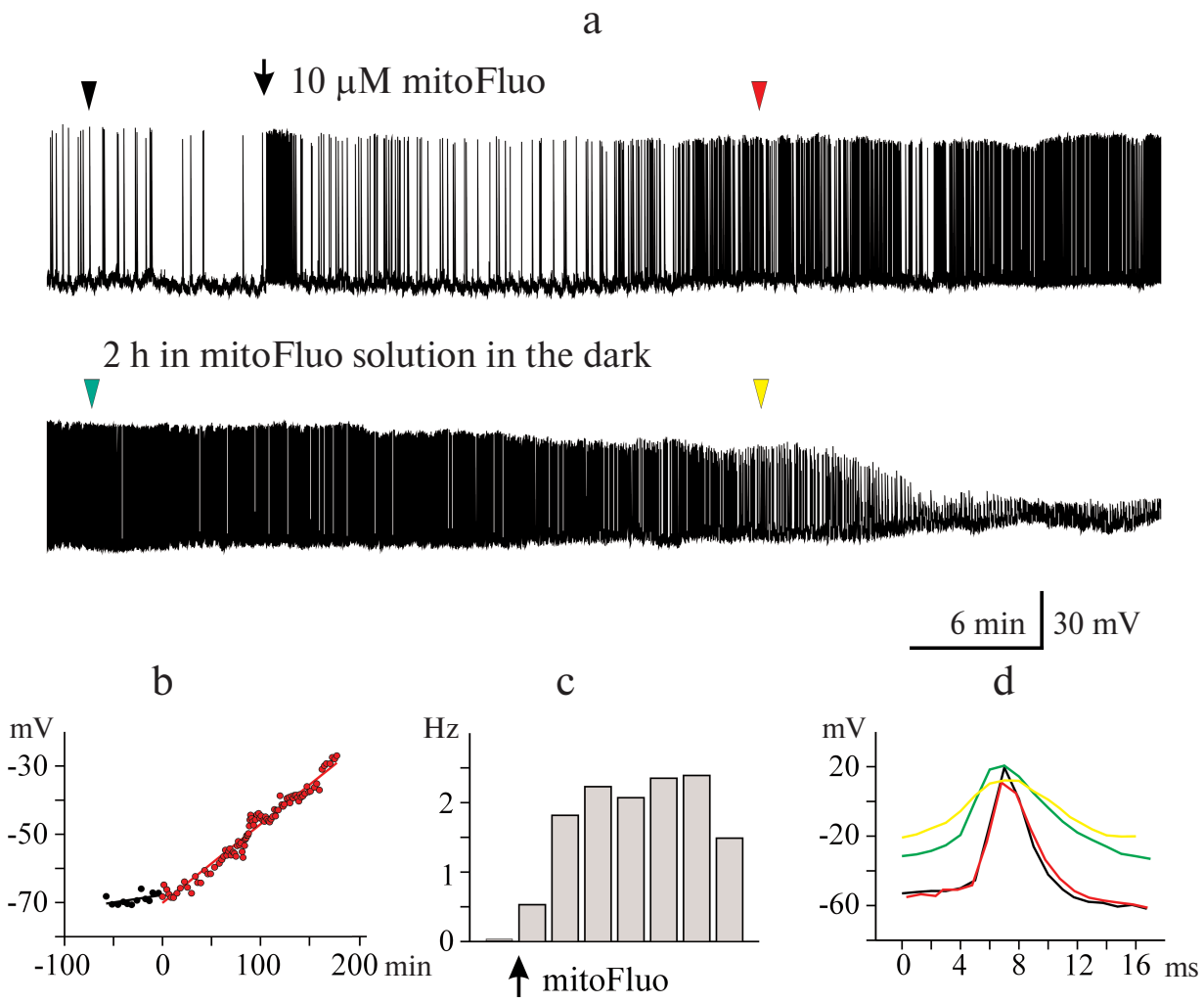

Fig. 4. MitoFluo at high concentrations causes complete inhibition of spontaneous activity of pond snail neurons. a) MitoFluo at a concentration of 10 μM causes depolarization of the plasma membrane, an increase in the spike frequency, and a decrease in the spike amplitude of the buccal neuron B4. The decrease in the spike frequency started 2 h after addition of mitoFluo (panel (a), lower part). b) RMP increased gradually in the presence of mitoFluo over the course of the entire experiment. The moment of the mitoFluo addition was considered as time point 0. c) The average action potential frequency increased more than 2-fold in the presence of mitoFluo in comparison with the control. The histogram was constructed using 20-min time intervals. d) Superposition of action potentials; mitoFluo decreased the rates of spike depolarization and repolarization. Positions of the spikes in the recording presented in panel (a) are shown with arrowheads of the corresponding color. Control spike is shown in black.

of B4 cell (Fig. 4a). The neuronal activity significantly changed following a short period of time (~15 min) after the addition of mitoFluo (10 μM): the plasma membrane depolarization increased (Fig. 4b), the action potential frequency increased (from 0.03 to 2.3 Hz) (Fig. 4c), and the spike depolarization and repolarization slopes decreased significantly (Fig. 4d). The addition of mitoFluo eventually resulted in complete silencing of the buccal cell (Fig. 4a, lower panel). Gradual broadening of the spikes started simultaneously with the plasma membrane depolarization and reached the maximum prior to the cell silencing. On average, mitoFluo at the concentrations of 2 μM and higher caused membrane depolarization of buccal cells by 20% (from −54.56 ± 2.49 mV in the control to −43.43 ± 2.56 mV in the presence of mitoFluo) (paired *t*-test: $p < 0.001$; $n = 16$ cells; Table 3). The average spike amplitude in buccal cells decreased by 13.7%. The maximal spike depolarization and repolarization slopes decreased from 25.38 ± 3.96 and −13.39 ± 2.17 mV/ms, respectively, in the control to 15.94 ± 3.92 and −8.47 ± 1.89 mV/ms, respectively, in the presence of mitoFluo (paired *t*-test: $p = 0.006$ and 0.010, respectively). On average, the half-width of spike increased by 64% (Table 3). Hence, mitoFluo caused changes in the spike parameters that were qualitatively similar to those observed in the presence of CCCP (Fig. 2e and Table 1). The effect of mitoFluo (2-60 μM) was investigated in 17 CGCs (Table 4). On average, in the presence of

mitoFluo, the membrane potential of CGCs changed by 14%, the half-width of spike increased by 35% from 15.84 ± 1.41 to 21.43 ± 1.9 ms (paired *t*-test: $p = 0.002$). Higher mitoFluo concentrations (60 μM) caused complete inhibition of the CGC electrical activity (data not shown). Hence, CGCs are less sensitive to mitoFluo than buccal cells, as it was also observed for CCCP. The decreased susceptibility of the CGCs to the action of uncouplers is likely related to their serotonergic function, which is corroborated by the fact that pedal serotonergic neurons also demonstrated increased resistance to the action of uncouplers in our experiments (data not shown).

It must be mentioned that after washing out mitoFluo ($n = 3$), the neuronal activity did not restore to the control level within the observation period (from 30 min to 4 h).

Induction of calcium release from the mitochondria by mitoFluo. Based on the effects of CCCP and triclosan on the electrical activity of *L. stagnalis* neurons shown in [13], it was reasonable to believe that the mitoFluo-induced changes in the neuronal activity were associated with changes in the cytoplasmic calcium concentration playing an important role in the regulation of plasma membrane channels [23-25]. It has been shown [26-29] that protonophoric uncouplers induce the release of calcium ions from mitochondria by reversing the function of the electrogenic calcium uniporter mediating the membrane potential-driven accumulation of calcium in the mitochondrial matrix. The uncoupler-induced drop in the membrane potential leads to the mitochondrial calcium efflux [29]. Since mitoFluo exhibits bright fluorescence, we monitored calcium efflux from the rat liver mitochondria using a calcium-selective electrode, but not

Table 3. Effect of mitoFluo on buccal neurons (B1, B2, B4) in the isolated pond snail ganglia

Buccal neurons, $n = 16$	Control, mean ± standard error	mitoFluo, mean ± standard error	Paired Student's *t*-test or Wilcoxon *t*-test	Change in percent
Membrane potential (mV)	−54.56 ± 2.49	−43.43 ± 2.56	$p < 0.001$	depolarization by 20.4%
Spike amplitude (mV)	60.56 ± 2.51	52.28 ± 3.63	$p = 0.030$	decrease by 13.7%
Spike width at half maximum (ms)	7.12 ± 1.00	11.67 ± 1.94	$p < 0.001$	broadening by 64%
Maximum rate of spike depolarization (mV/ms)	25.38 ± 3.96	15.94 ± 3.92	$p = 0.006$	slowing down by 37%
Maximum rate of spike repolarization (mV/ms)	−13.39 ± 2.17	−8.47 ± 1.89	$p = 0.010$	slowing down by 36.7%
Average spike frequency (Hz)	1.68 ± 0.44	3.30 ± 0.65	$p < 0.001$	increase by 96%

Table 4. Effect of mitoFluo on CGCs in the isolated pond snail ganglia

CGC, $n = 17$	Control, mean ± standard error	mitoFluo, mean ± standard error	Paired Student's *t*-test or Wilcoxon *t*-test	Change in percent
Membrane potential (mV)	−55.78 ± 8.44	−48.17 ± 8.22	$p < 0.001$	depolarization by 14%
Spike amplitude (mV)	78.70 ± 2.08	75.08 ± 2.72	$p = 0.006$	decrease by 5%
Spike width at half maximum (ms)	15.84 ± 1.41	21.43 ± 1.90	$p = 0.002$	broadening by 35%
Maximum rate of spike depolarization (mV/ms)	22.74 ± 2.27	17.52 ± 1.66	$p = 0.002$	slowing down by 23%
Maximum rate of spike repolarization (mV/ms)	−7.55 ± 0.80	−5.35 ± 0.40	$p = 0.007$	slowing down by 30%
Average spike frequency (Hz)	0.59 ± 0.06	0.83 ± 0.05	$p < 0.001$	increase by 42%

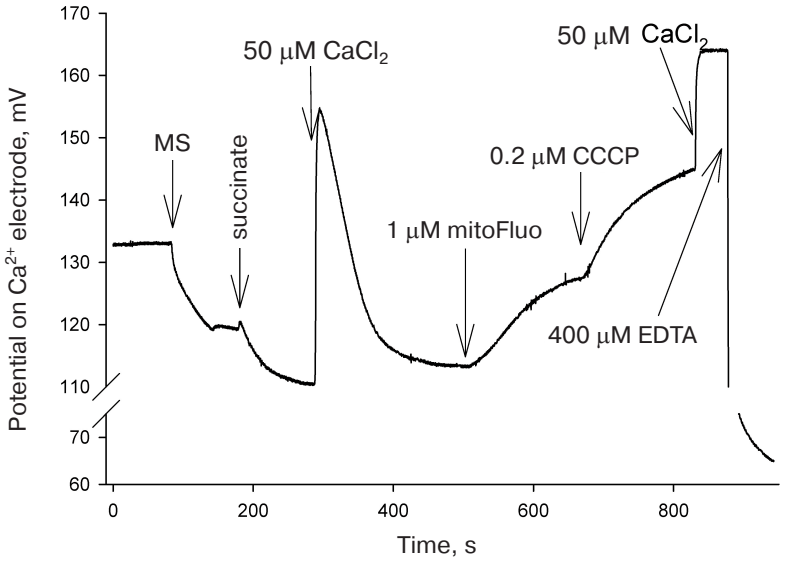

Fig. 5. Calcium efflux from the rat liver mitochondria upon addition of mitoFluo and CCCP recorded with a calcium-selective electrode. The moments of mitoFluo and CCCP addition are marked with arrows. Reagents: 2 mM succinate, 50 μM Ca^{2+}, 1 μM mitoFluo, 200 nM CCCP, 400 μM EDTA, 1 mg/ml mitochondria suspension (MS). Medium: 250 mM sucrose, 20 mM Tris, 10 mM KH_2PO_4, 1 mM $MgCl_2$.

calcium-sensitive fluorescent probes (Fig. 5). The addition of mitoFluo to the buffer solution containing isolated rat liver mitochondria resulted in an increase in the calcium concentration in the medium due to its release from the mitochondria; the CCCP addition to the medium produced the same effect.

Photoinduced effect of mitoFluo on the electrical activity of pond snail neurons. The photoinduced effect of mitoFluo was investigated in nine experiments by recording the activity of 10 CGCs, 13 buccal cells, and one pedal neuron. The representative recordings of the activity of buccal neurons B1 and B4 and CGC after the addition of 7 μM mitoFluo in the dark are shown in Fig. 6a. Illumination of the ganglia caused fast changes in their activity manifesting as membrane depolarization (Fig. 6b) and an increase in the spike frequency (Fig. 6c, green bars). Note that the B4 cell, which was silent prior to illumination, responded by rapid excitation. The pattern of the buccal cell activity also changed – a normal fictive feeding rhythm disappeared completely. The short-term membrane hyperpolarization was observed in several cells prior to depolarization. Illumination of the ganglia affected the shape of the spikes. The amplitude of the spikes decreased, and the spikes broadened in the course of membrane depolarization (Fig. 6d). Finally, illumination in the presence of mitoFluo blocked the ability of neurons to generate the action potential.

It is reasonable to suggest that the effect of illumination on the electrical activity of pond snail neurons in the presence of mitoFluo can be explained by the photodynamic effect of mitoFluo as a photosensitizer. Indeed, it is known that fluorescein can generate singlet oxygen in aqueous solutions, although with a very low quantum yield of ~0.06 [30]. It was also shown that a conjugate of fluorescein with cAMP was capable of modifying cAMP-dependent channels in response to illumination via the photodynamic mechanism [31].

In order to test the photodynamic nature of the light-induced effect of mitoFluo on the electrical activity of neurons, we conducted analogous experiments with the classical photosensitizer Rose Bengal. The activity of 7 CGCs and 3 buccal cells was recorded in four experiments. Figure 7 shows that illumination in the presence of Rose Bengal causes fast depolarization of the plasma membrane and eventual suppression of the electrical activity that was preceded by a significant increase in the spike frequency in the B4 neurons and CGCs. It is interesting to note that illumination of the isolated pond snail ganglia by itself did not affect the membrane potential (Fig. 7b) and spike frequency (Fig. 7c), while illumination in the presence of Rose Bengal changed these parameters immediately (within seconds) and irreversibly (Fig. 7d). The shape of the spikes also changed (Fig. 7e). Hence, the photoinduced effects of Rose Bengal and mitoFluo on the electrical activity of snail neurons were essentially similar, but the time of the neuron response significantly differed for these two compounds.

Photodynamic effect of mitoFluo on gramicidin A-induced ion channels. The ability of mitoFluo to act as a photosensitizer was studied in the system previously developed in our laboratory that involved photoinactivation of the gramicidin A-induced ion channels in a planar BLM [32-35]. The representative recording of the current across the BLM induced by the addition of 2 nM grami-

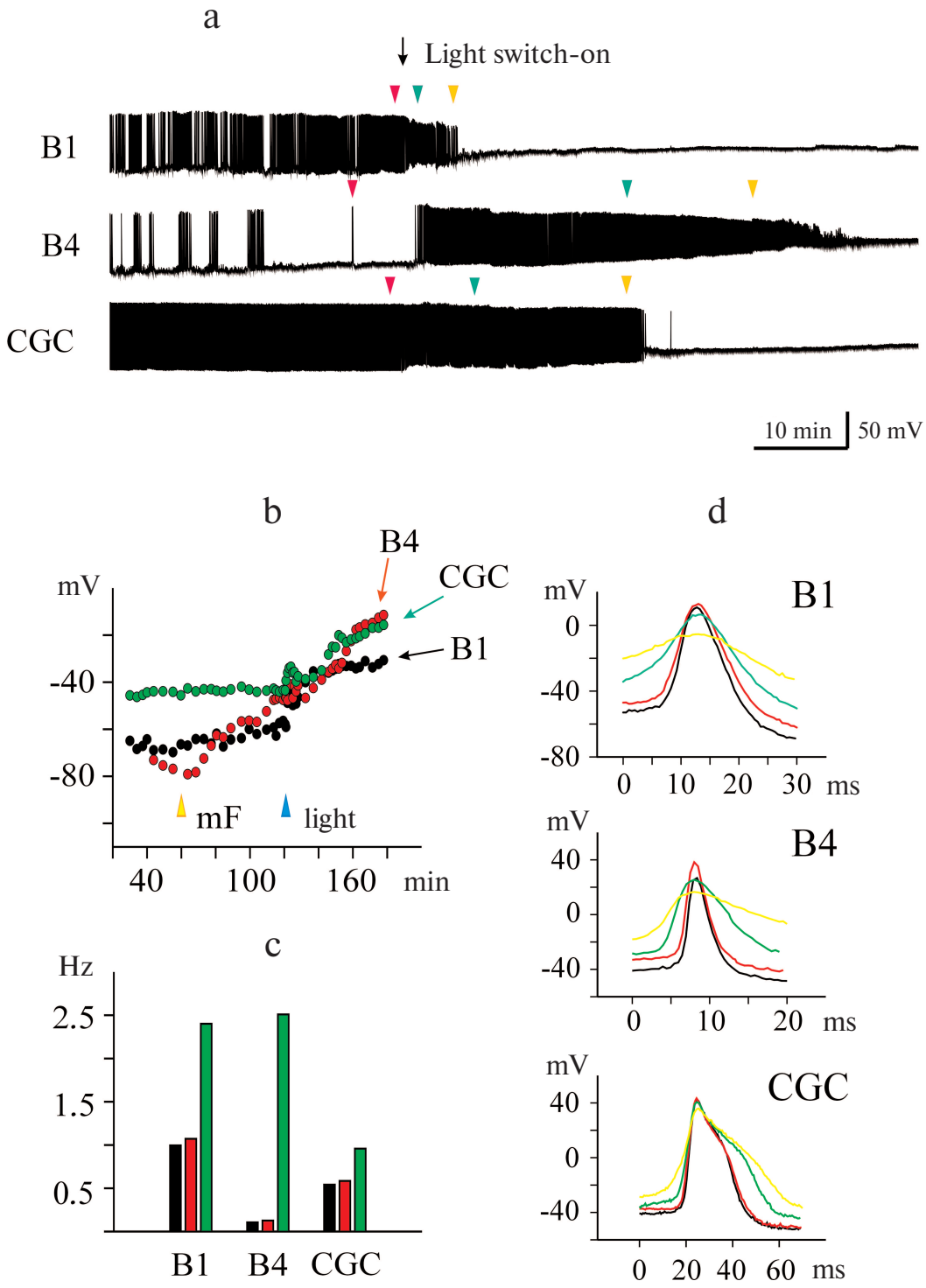

Fig. 6. Photoinduced changes in spontaneous activity of pond snail neurons in the presence of mitoFluo. a) Illumination of ganglia in the presence of 7 μM mitoFluo caused depolarization of the membrane of the buccal neurons B1 and B4 and CGC and affected the amplitude and frequency of the action potential. The excitation phase was replaced with the inhibition of spike activity, which developed at different rate in different neurons. b) The addition of mitoFluo (yellow arrowhead) resulted in an increase in the RMP of the buccal cells, but only slightly affected the RMP in the CGC. Illumination (blue arrowhead) resulted in significant depolarization of all three cells. c) Illumination in the presence of 7 μM mitoFluo increased the average spike frequency. Black, red, and green bars, average spike frequency in the control, in the presence of mitoFluo, and upon illumination, respectively. d) Effect of illumination in the presence of mitoFluo on the spike shape for all three neurons. Control spike is shown in black. Positions of the spikes in the recording presented in panel (a) are indicated with arrowheads of the corresponding color.

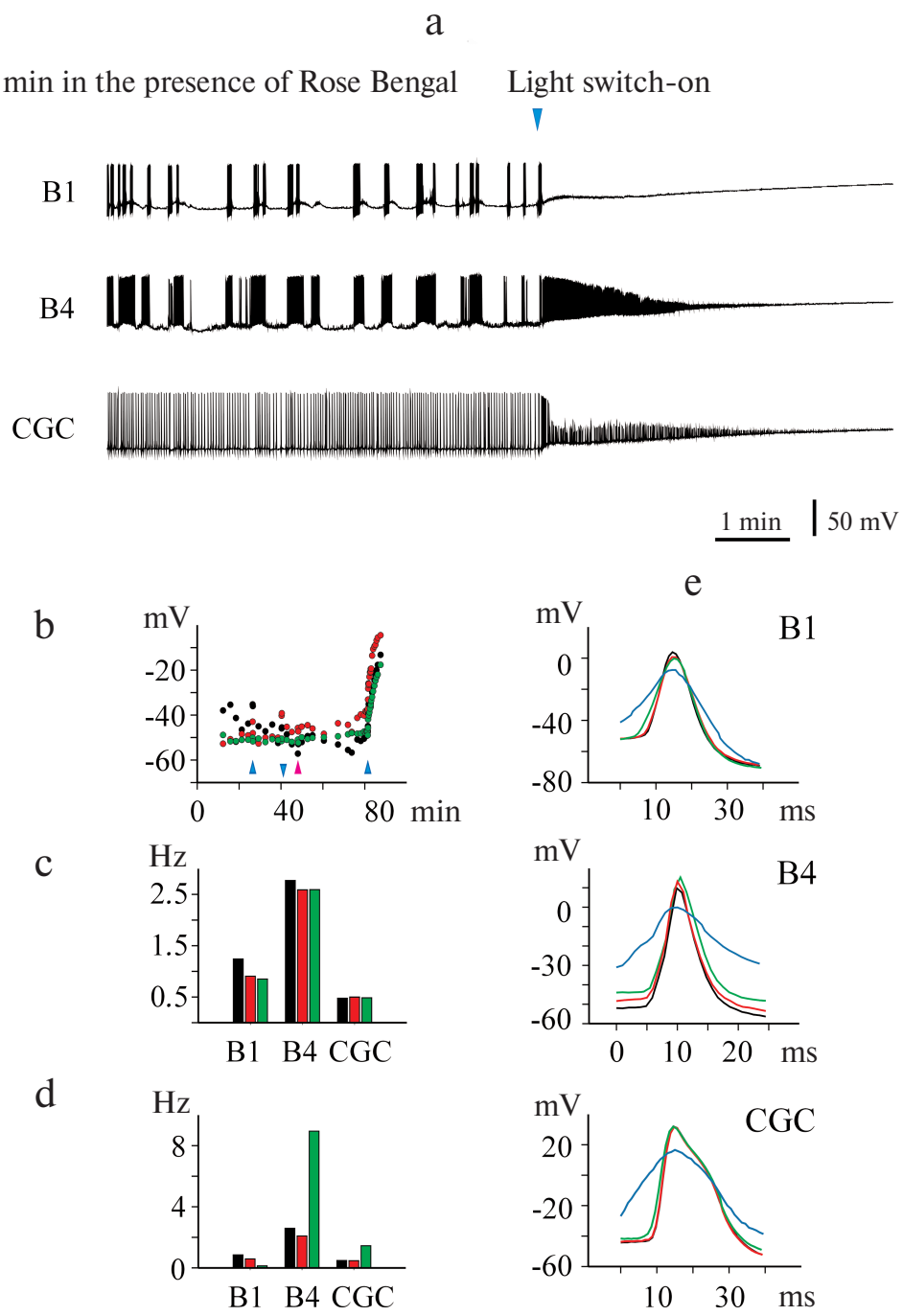

Fig. 7. Photoinduced changes in spontaneous activity of pond snail neurons in the presence of Rose Bengal. a) Illumination of ganglia in the presence of 1 μM Rose Bengal caused rapid membrane depolarization and silencing of neurons within 1-2 min. b) Illumination of the ganglia in the absence of additions did not affect the membrane potential, while switching on the light (blue arrowheads) in the presence of Rose Bengal caused rapid membrane depolarization in all three investigated cells. The addition of Rose Bengal is indicated with pink arrowhead. c) Illumination of ganglia did not significantly affect the average action potential frequency. Black, red, and green correspond to the average spike frequency in the dark, upon illumination, and after switching off the light, respectively. d) The addition of Rose Bengal (1 μM, red bars) only slightly affected the average frequency of action potential generation in comparison with the control (black bars). Illumination in the presence of Rose Bengal (green bars) caused a significant increase in the average frequency of spike generation in the B4 neurons and CGC. The B1 neuron became silent immediately after switching on the light (see also Fig. 7a). e) Superposition of the action potentials of the B1 and B4 neurons and CGC. Black, red, green, and blue correspond to the spikes observed in the dark (control), upon illumination, in the presence of Rose Bengal without illumination, and in the presence of Rose Bengal upon illumination, respectively. The photoinduced effect of Rose Bengal on the spike shape in all three neurons developed within a second time scale.

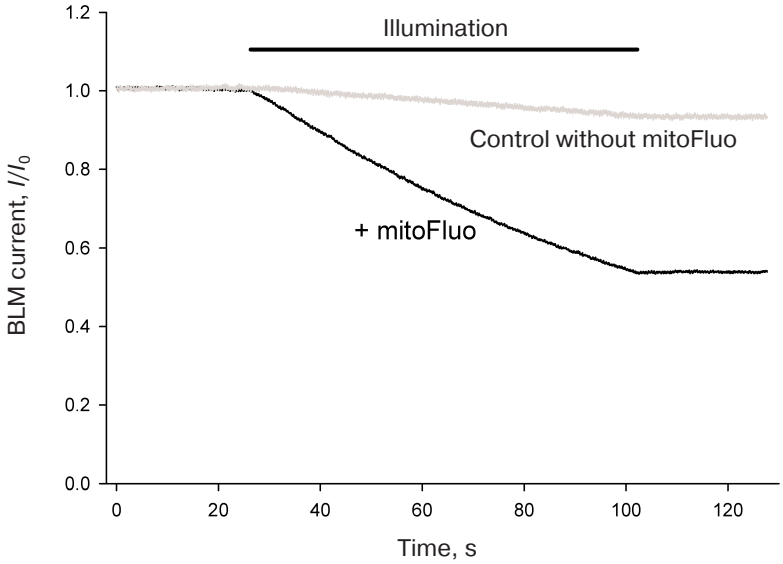

Fig. 8. Kinetics of the relative current (I/I_0) upon the BLM illumination with white light (illumination time period is shown by the line above the figure) in the presence (black) or absence (grey) of 1 μM of mitoFluo. BLM was formed from DPhPC. The membrane current (I_0) was 0.3 μA.

cidin A to the 100 mM KCl solution, pH 7.0, bathing the membrane, is presented in Fig. 8a. The membrane was illuminated with white light for the time period marked with black line. No changes in the current through the BLM were observed under illumination in the absence of mitoFluo (curve *1*), while illumination in the presence of mitoFluo (curve *2*) caused a noticeable drop in the current through the gramicidin A channels. The decrease in the current was less pronounced when 10 mM sodium azide (singlet oxygen quencher) was added to the medium (data not shown).

It should be mentioned that the data on a decrease in the spike amplitude, broadening of the spikes [36-39], and an increase in the spike frequency [40-43] in the excitable cells subjected to the action of photodynamic agents have been long reported in the literature. Taking into consideration an increase in the cytoplasmic calcium concentration in response to the photodynamic action [44] and stimulation of the spike activity by increasing the cytoplasmic calcium [24, 25, 45], the changes in the parameters of the electrical activity of *L. stagnalis* neurons observed in this study upon illumination of the cells after prolonged incubation with mitoFluo can be explained by the influx of calcium ions into the cytoplasm from the endoplasmic reticulum, which was mediated by ROS formed as a result of dye excitation with light. Formation of lipid peroxidation products during prolonged illumination of cell homogenates in the presence of fluorescein was demonstrated in [46]. It is known that changes in the intracellular calcium concentration modulate the functions of various types of ion channels in the plasma membrane, thus affecting the membrane potential, generation of the action potential, and other processes. In particular, it was shown that an increase in the intracellular calcium results in the inactivation of calcium channels in *L. stagnalis* neurons [23]. Considering the mechanism of light-induced effect of mitoFluo on the activity of *L. stagnalis* neurons, one cannot rule out the possibility of photoinduced modification of proteins forming ion channels, as it was suggested in the study of the photochemical modification of sodium currents in the lobster giant axons [47]. The above-described photodynamic inactivation of gramicidin A-induced channels in the BLM is an example of the effect of light on ion channels in the presence of a photosensitizer.

Funding. This work was supported by the Russian Science Foundation (project 16-14-10025).

Conflict of interest. The authors declare no conflict of interest in financial or any other sphere.

Ethical approval. All applicable international, national, and/or institutional guidelines for the care and use of laboratory animals were followed in this study.

REFERENCES

1. Korde, A. S., Pettigrew, L. C., Craddock, S. D., and Maragos, W. F. (2005) The mitochondrial uncoupler 2,4-dinitrophenol attenuates tissue damage and improves mitochondrial homeostasis following transient focal cerebral ischemia, *J. Neurochem.*, **94**, 1676-1684; doi: 10.1111/j.1471-4159.2005.03328.x.

2. Silachev, D. N., Khailova, L. S., Babenko, V. A., Gulyaev, M. V., Kovalchuk, S. I., Zorova, L. D., Plotnikov, E. Y., Antonenko, Y. N., and Zorov, D. B. (2014) Neuroprotective effect of glutamate-substituted analog of gramicidin A is mediated by the uncoupling of mitochondria, *Biochim. Biophys. Acta*, **1840**, 3434-3442; doi: 10.1016/j.bbagen.2014.09.002.
3. Khailova, L. S., Silachev, D. N., Rokitskaya, T. I., Avetisyan, A. V., Lyamzaev, K. G., Severina, I. I., Il'yasova, T. M., Gulyaev, M. V., Dedukhova, V. I., Trendeleva, T. A., Plotnikov, E. Y., Zvyagilskaya, R. A., Chernyak, B. V., Zorov, D. B., Antonenko, Y. N., and Skulachev, V. P. (2014) A short-chain alkyl derivative of rhodamine 19 acts as a mild uncoupler of mitochondria and a neuroprotector, *Biochim. Biophys. Acta*, **1837**, 1739-1747; doi: 10.1016/j.bbabio.2014.07.006.
4. Antonenko, Y. N., Denisov, S. S., Silachev, D. N., Khailova, L. S., Jankauskas, S. S., Rokitskaya, T. I., Danilina, T. I., Kotova, E. A., Korshunova, G. A., Plotnikov, E. Y., and Zorov, D. B. (2016) A long-linker conjugate of fluorescein and triphenylphosphonium as mitochondria-targeted uncoupler and fluorescent neuro- and nephroprotector, *Biochim. Biophys. Acta*, **1860**, 2463-2473; doi: 10.1016/j.bbagen.2016.07.014.
5. Boveris, A. (1977) Mitochondrial production of superoxide radical and hydrogen peroxide, *Adv. Exp. Med. Biol.*, **78**, 67-82.
6. Korshunov, S. S., Skulachev, V. P., and Starkov, A. A. (1997) High protonic potential actuates a mechanism of production of reactive oxygen species in mitochondria, *FEBS Lett.*, **416**, 15-18.
7. Liu, S. S. (1997) Generating, partitioning, targeting and functioning of superoxide in mitochondria, *Biosci. Rep.*, **17**, 259-272.
8. McLaughlin, S. G., and Dilger, J. P. (1980) Transport of protons across membranes by weak acids, *Physiol. Rev.*, **60**, 825-863; doi: 10.1152/physrev.1980.60.3.825.
9. Liberman, E. A., Topaly, V. P., Tsofina, L. M., Jasaitis, A. A., and Skulachev, V. P. (1969) Mechanism of coupling of oxidative phosphorylation and the membrane potential of mitochondria, *Nature*, **222**, 1076-1078.
10. Terada, H. (1990) Uncouplers of oxidative phosphorylation, *Environ. Health Perspect.*, **87**, 213-218; doi: 10.1289/ehp.9087213.
11. Shchepinova, M. M., Denisov, S. S., Kotova, E. A., Khailova, L. S., Knorre, D. A., Korshunova, G. A., Tashlitsky, V. N., Severin, F. F., and Antonenko, Y. N. (2014) Dodecyl and octyl esters of fluorescein as protonophores and uncouplers of oxidative phosphorylation in mitochondria at submicromolar concentrations, *Biochim. Biophys. Acta*, **1837**, 149-158; doi: 10.1016/j.bbabio.2013.09.011.
12. Denisov, S. S., Kotova, E. A., Plotnikov, E. Y., Tikhonov, A. A., Zorov, D. B., Korshunova, G. A., and Antonenko, Y. N. (2014) A mitochondria-targeted protonophoric uncoupler derived from fluorescein, *Chem. Commun.*, **50**, 15366-15369; doi: 10.1039/c4cc04996a.
13. Popova, L. B., Nosikova, E. S., Kotova, E. A., Tarasova, E. O., Nazarov, P. A., Khailova, L. S., Balezina, O. P., and Antonenko, Y. N. (2018) Protonophoric action of triclosan causes calcium efflux from mitochondria, plasma membrane depolarization and bursts of miniature end-plate potentials, *Biochim. Biophys. Acta Biomembr.*, **1860**, 1000-1007; doi: 10.1016/j.bbamem.2018.01.008.
14. Doebler, J. A. (2000) Effects of protonophores on membrane electrical characteristics in NG108-15 cells, *Neurochem. Res.*, **25**, 263-268.
15. Tretter, L., Chinopoulos, C., and Adam-Vizi, V. (1998) Plasma membrane depolarization and disturbed Na^+ homeostasis induced by the protonophore carbonyl cyanide-*p*-trifluoromethoxyphenylhydrazone in isolated nerve terminals, *Mol. Pharmacol.*, **53**, 734-741.
16. Benjamin, P. R., and Rose, R. M. (1979) Central generation of bursting in the feeding system of the snail *Lymnaea stagnalis*, *J. Exp. Biol.*, **80**, 93-118.
17. McCrohan, C. R., and Benjamin, P. R. (1980) Patterns of activity and axonal projections of the cerebral giant cells of the snail *Lymnaea stagnalis*, *J. Exp. Biol.*, **85**, 149-168.
18. Johnson, D., and Lardy, H. (1967) Isolation of liver or kidney mitochondria, *Methods Enzymol.*, **10**, 94-96.
19. Mueller, P., Rudin, D. O., Tien, H. T., and Wescott, W. C. (1963) Methods for the formation of single bimolecular lipid membranes in aqueous solution, *J. Phys. Chem.*, **67**, 534-535.
20. Zhao, Z., Gordan, R., Wen, H., Fefelova, N., Zang, W.-J., and Xie, L.-H. (2013) Modulation of intracellular calcium waves and triggered activities by mitochondrial Ca flux in mouse cardiomyocytes, *PLOS ONE*, **8**, e80574, doi: 10.1371/journal.pone.0080574.
21. Bulbring, E., and Lullmann, H. (1957) The effect of metabolic inhibitors on the electrical and mechanical activity of the smooth muscle of the guinea-pig's "taenia coli", *J. Physiol.*, **136**, 310-323.
22. Krnjevic, K., Puil, E., and Werman, R. (1978) Significance of 2,4-dinitrophenol action on spinal motoneurons, *J. Physiol.*, **275**, 225-239.
23. Byerly, L., and Moody, W. J. (1984) Intracellular calcium ions and calcium currents in perfused neurons of the snail *Lymnaea stagnalis*, *J. Physiol.*, **352**, 637-652.
24. Tse, A., and Hille, B. (1992) GnRH-induced Ca^{2+} oscillations and rhythmic hyperpolarizations of pituitary gonadotropes, *Science*, **255**, 462-464.
25. Stojilkovic, S. S. (2012) Molecular mechanisms of pituitary endocrine cell calcium handling, *Cell Calcium*, **51**, 212-221; doi: 10.1016/j.ceca.2011.11.003.
26. Carafoli, E. (1967) *In vivo* effect of uncoupling agents on the incorporation of calcium and strontium into mitochondria and other subcellular fractions of rat liver, *J. Gen. Physiol.*, **50**, 1849-1864.
27. Rottenberg, H., and Scarpa, A. (1974) Calcium uptake and membrane potential in mitochondria, *Biochemistry*, **13**, 4811-4817.
28. Gunter, T. E., Gunter, K. K., Puskin, J. S., and Russell, P. R. (1978) Efflux of Ca^{2+} and Mn^{2+} from rat liver mitochondria, *Biochemistry*, **17**, 339-345.
29. Bernardi, P., Paradisi, V., Pozzan, T., and Azzone, G. F. (1984) Pathway for uncoupler-induced calcium efflux in rat liver mitochondria: inhibition by ruthenium red, *Biochemistry*, **23**, 1645-1651.
30. Usui, Y. (1973) Determination of quantum yield of singlet oxygen formation by photosensitization, *Chem. Lett.*, **2**, 743-744.
31. Gao, W., Su, Z., Liu, Q., and Zhou, L. (2014) State-dependent and site-directed photodynamic transformation

of HCN2 channel by singlet oxygen, *J. Gen. Physiol.*, **143**, 633-644; doi: 10.1085/jgp.201311112.
32. Rokitskaya, T. I., Antonenko, Y. N., and Kotova, E. A. (1996) Photodynamic inactivation of gramicidin channels: a flash-photolysis study, *Biochim. Biophys. Acta*, **1275**, 221-226.
33. Rokitskaya, T. I., Block, M., Antonenko, Y. N., Kotova, E. A., and Pohl, P. (2000) Photosensitizer binding to lipid bilayers as a precondition for the photoinactivation of membrane channels, *Biophys. J.*, **78**, 2572-2580; doi: 10.1016/S0006-3495(00)76801-9.
34. Antonenko, Y. N., Kotova, E. A., and Rokitskaya, T. I. (2005) Photodynamic effect as a basis of relaxation method of the study of gramicidin channels, *Biol. Membr. (Moscow)*, **22**, 275-289.
35. Pashkovskaya, A. A., Sokolenko, E. A., Sokolov, V. S., Kotova, E. A., and Antonenko, Y. N. (2007) Photodynamic activity and binding of sulfonated metallophthalocyanines to phospholipid membranes: contribution of metal-phosphate coordination, *Biochim. Biophys. Acta*, **1768**, 2459-2465; doi: 10.1016/j.bbamem.2007.05.018.
36. Lyudkovskaya, R. G. (1961) Some peculiarities of the squid giant axon excitation with light, *Biofizika*, **6**, 300-308.
37. Pooler, J. (1968) Light-induced changes in dye-treated lobster giant axons, *Biophys. J.*, **8**, 1009-1026.
38. Pooler, J. (1972) Photodynamic alteration of sodium currents in lobster axons, *J. Gen. Physiol.*, **60**, 367-387.
39. Oxford, G. S., Pooler, J. P., and Narahashi, T. (1977) Internal and external application of photodynamic sensitizers on squid giant axons, *J. Membr. Biol.*, **36**, 159-173.
40. Burmistrov, Yu. M., Lyudkovskaya, R. G., and Shuranova, Zh. P. (1969) Electrical activity of the neurons of the crayfish on vital staining with methylene blue, *Biofizika*, **14**, 495-500.
41. Pooler, J., and Oxford, G. S. (1973) Photodynamic alteration of lobster giant axons in calcium-free and calcium-rich media, *J. Membr. Biol.*, **12**, 339-348.
42. Kress, M., Petersen, M., and Reeh, P. W. (1997) Methylene blue induces ongoing activity in rat cutaneous primary afferents and depolarization of DRG neurons via a photosensitive mechanism, *Naunyn Schmiedebergs Arch. Pharmacol.*, **356**, 619-625.
43. Uzdensky, A., Bragin, D., Kolosov, M., Dergacheva, O., Fedorenko, G., and Zhavoronkova, A. (2002) Photodynamic inactivation of isolated crayfish mechanoreceptor neuron: different death modes under different photosensitizer concentrations, *Photochem. Photobiol.*, **76**, 431-437.
44. Neginskaya, M., Berezhnaya, E., Uzdensky, A. B., and Abramov, A. Y. (2018) Reactive oxygen species produced by a photodynamic effect induced calcium signal in neurons and astrocytes, *Mol. Neurobiol.*, **55**, 96-102; doi: 10.1007/s12035-017-0721-1.
45. Grace, A. A., and Bunney, B. S. (1984) The control of firing pattern in nigral dopamine neurons: burst firing, *J. Neurosci.*, **4**, 2877-2890.
46. Hiramitsu, T., Miura, Y., and Machida, H. (1992) Photosensitizer-induced lipid peroxidation in retinal homogenates under illumination, *J. Clin. Biochem. Nutr.*, **12**, 109-114.
47. Pooler, J. P., and Valenzeno, D. P. (1978) Kinetic factors governing sensitized photooxidation of excitable cell membranes, *Photochem. Photobiol.*, **28**, 219-226.